Vol. 61: 93–107, 2014
doi: 10.3354/cr01241

CLIMATE RESEARCH
Clim Res

Published September 23

Rainfall and climate variability: long-term trends in the Metropolitan Area of São Paulo in the 20th century

Guillermo O. Obregón[1,*], José A. Marengo[1], Carlos A. Nobre[2]

[1]Earth System Science Center, National Institute for Space Research (CCST/INPE), Rodovia Presidente Dutra, km 39, 12630-000, Cachoeira Paulista, São Paulo, Brazil

[2]Research and Development Policies and Programs Secretary, Ministry of Science, Technology and Innovation (SEPED/MCTI), Bloco E, 2º andar, Sala 215, Esplanada dos Ministérios, 12227-010, Brasília-DF, Brazil

ABSTRACT: We investigated spatial–temporal variability and long-term trends of rainfall over the Metropolitan Area of São Paulo (MASP). Due to a lack of continuous and consistent rainfall observations in the MASP, a database for the spatial analysis was created from a composite of 94 stations, with daily rainfall data for 1973–1997, plus data from the University of São Paulo's Institute of Geophysics and Astronomy (IAG/USP) station for 1933–2011, as the base of the long-term variability analysis. It is shown that the seasonal and interannual rainfall variability result from underlying local influences and remote large-scale atmospheric dynamics. These effects appear to be more complex during the austral spring and fall seasons, and seem to determine the duration of the rainy period over the MASP. The intraseasonal (30–60 d) oscillation of rainfall does not exhibit any long-term modulation; interannual rainfall variability for 1975–1990 appears modulated by the El Niño–Southern Oscillation (ENSO) scale (2–8 yr). Nonetheless, there exists statistical evidence that the rainfall climate over the MASP had an abrupt change at the end of the 1950s, but the global climatic change that occurred in the middle of the 1970s is not evident. The progressive increase in the frequency of rainy days and total daily rainfall throughout the period of analysis are prominent factors in the trend of annual and seasonal rainfall. Furthermore, rainfall variability over the MASP may be modulated by the Southern Annular Mode (SAM), Pacific Decadal Oscillation (PDO) and ENSO at seasonal scales, altering the normal progression of the seasonal rainfall cycle, while at interannual scales, each one of these patterns drives the rainfall variability, mainly when each pattern reaches its extreme value.

KEY WORDS: Metropolitan Area of São Paulo · Rainfall variability · Abrupt rainfall change · Rainfall trends

1. INTRODUCTION

The city of São Paulo, the capital of the state of the same name, located in southeastern Brazil, underwent intense urban development during the 20th century, and with continuous urban population growth, it became the largest city in Brazil by the 1950s. Consequently, population growth combined with urban expansion led to the development of a large area with features of a megacity: the Metropolitan Area of São Paulo (MASP). With nearly 20 million inhabitants (IBGE 2011) and an area of some 8000 km^2, the MASP is the largest urban agglomeration in Brazil and among the 10 largest in the world.

As in many other urban regions of the world, rainfall variability (especially the frequency and duration of heavy rainfall events) is currently becoming the largest source of risk for the population (Parry et al. 2007, Pall et al. 2011). Additionally, given the evidence of climate change, megacities will become the areas most vulnerable to the impacts of more intense and frequent extreme rainfall events (Katz & Brown 1992) and their effects, such as floods and violent landslides. Consequently, an increase in rainfall and

*Corresponding author: guillermo.obregon@inpe.br

its extremes are affecting human life in the MASP, both in the present and in the coming decades. In this sense, it is critical to understand the underlying dynamics of climate variability in its various spatial–temporal scales in the MASP, so that climate vulnerability may be assessed and adaptation strategies proposed. This can serve to reduce the risks of climate change impacts, since decisions and policies must be determined by taking climate variability into account (Ahmed & Sanchez 2008, Marquina 2010).

Rainfall variability, from daily to interannual and decadal timescales, is governed by large-scale weather patterns. Therefore, interactions between local and synoptic scales, influenced by large-scale patterns, have always modulated urban rainfall in areas such as the MASP (Barros 1994, Magaña et al. 2003). Sometimes large-scale weather conditions are the dominant influences, whereas local conditions prevail in others (Landsberg 1981). In this context, Xavier et al. (1994), using daily rainfall data collected in the MASP during 1933–1986, point out a complex interaction between the local scale (urban effect) and the synoptic scale (natural effects). Furthermore, large-scale cold fronts appear as the principal factor in producing rain in the MASP during the dry season (Reboita et al. 2010). In fact, many studies that have dealt with variability in precipitation, especially episodes of severe storms that have occurred in the MASP, suggest that the physical mechanisms responsible for the occurrence of these events are related to, among other factors: frontal systems (Pereira Filho et al. 2002); the South Atlantic Convergence Zone (SACZ) (Silveira & Silva Dias 1990); and the urban heat island associated with the penetration of sea breezes (Pereira Filho et al. 2004, Freitas et al. 2007, Marengo et al. 2009). Also, intraseasonal rainfall variability is greater during the wet season (Carvalho et al. 2004) and appears to be strongly linked to SACZ activity (Paegle et al. 2000).

On interannual timescales, the effect of the El Niño–Southern Oscillation (ENSO) phenomenon on rainfall variability in the MASP is weak. Only intense ENSO events affect rainfall in the MASP during autumn (Kane 2000), increasing the amount of rainfall from April to May and altering the spatial distribution in the a north–south direction during May (Xavier et al. 1995). Silva Dias et al. (2013) mention that ENSO events have little connection with the extreme daily rainfall events seen in the MASP, whereas the Pacific Decadal Oscillation (PDO) and the North Atlantic Oscillation (NAO) explain much of the rainfall variability, especially in the dry season.

Several studies have shown a worldwide increase in heavy rainfall (e.g. Groisman et al. 2005, Alexander et al. 2006, Min et al. 2011, Donat et al. 2013, Westra et al. 2013). In southeastern Brazil, intense rainfall episodes are more frequent and associated with an increase in the number of consecutive dry days (Dufek & Ambrizzi 2007, Marengo et al. 2009, 2013). Extreme daily rainfall and the frequency of the number of days with heavy precipitation have increased in recent decades (Sugahara et al. 2009, Nobre et al. 2010, Marengo et al. 2013, Silva Dias et al. 2013).

The rainfall variability characteristics observed in the MASP are a complex response to various nonlinear and non-local physical and dynamic processes. These influence rainfall as a result of the interaction between the different components of the climate system, which have their own temporal characteristics. Because previous studies on rainfall variability in the MASP have not taken spatial variability (over the entire domain) and various time scales into account, a more comprehensive study of spatial and temporal rainfall analysis over the MASP is needed.

Therefore, this study is directed toward (1) examination of spatial–temporal rainfall variability observed, highlighting seasonal and annual scales; and (2) investigation of temporal variability at several time scales, from the intraseasonal variability to long-term trends, based on rainfall data from the University of São Paulo's Institute of Geophysics and Astronomy (IAG/USP) station for the period 1933–2011. In addition, it is expected that this study will provide some knowledge about rainfall variability in the MASP, and aid understanding of the spatial–temporal relationships between the physical and dynamic processes that generate rainfall at different scales.

2. METHODS

2.1. Study area and database construction

MASP is a megacity located in the southeast of Brazil, between 23.2–24.1° S and 45.7–47.2° W (Fig. 1), covering about 8000 km^2. The southern side of the MASP is bordered by the slopes of the Serra do Mar mountains, and the northeastern (northwestern) side lies on the eastern (western) edge of the Serra da Cantareira (Paranapiacaba) mountain range. Two rainfall datasets were selected from the database of the daily rainfall series collected at rainfall stations scattered over the MASP by the Department of Water

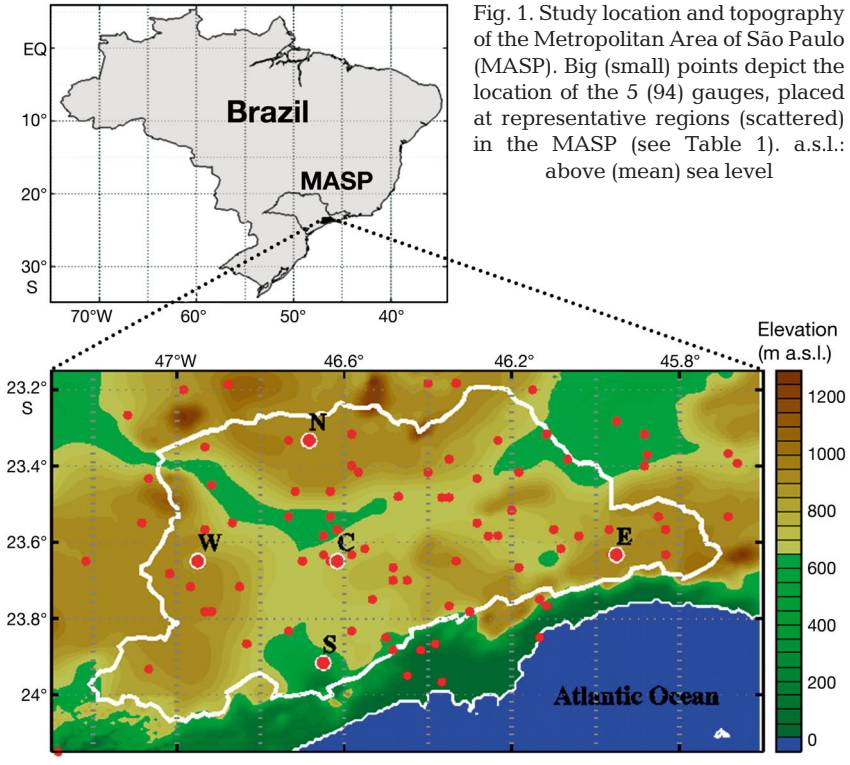

Fig. 1. Study location and topography of the Metropolitan Area of São Paulo (MASP). Big (small) points depict the location of the 5 (94) gauges, placed at representative regions (scattered) in the MASP (see Table 1). a.s.l.: above (mean) sea level

and Energy (DAEE) of the State of São Paulo, the National Water Agency (ANA) and the IAG/USP. The quality of the rainfall data and the limited spatial–temporal coverage of the available daily rainfall series makes it more difficult to meet the requirement of homogeneity of both spatial and temporal data necessary for the kind of analysis proposed here. The solution chosen to circumvent this dilemma was to collect all the available data over the MASP (110 stations) for the period 1933–2002 and identify the time window with the highest number of functioning rainfall stations, following the methodology used by Ronchi et al. (2007). The period chosen was 1973–1997 (25 yr). Then, in order to produce a usable dataset, we checked all rainfall data from this period to eliminate obvious data errors and inconsistencies, and then we worked on the more complexes analyses, trying to separate good- and bad-quality data. The steps, following Einfalt & Michaelides (2008), were (1) completness: detection of gaps in the data; (2) extreme values: detection of the physically impossible values; (3) variability: control of measurement variability; (4) physical processes behind the measured parameter: detection of constant values; and (5) control of spatial consistency: comparing measurements of the same parameters from different stations. After this, the inconsistencies of rainfall data found in a few time series were removed; missing data were not filled in. Therefore, the main database for spatial analysis includes daily rainfall time series for 94 stations spread over the MASP and surrounding areas with missing values for ≤8% (not continuous) of the period 1973–1997 (25 yr). The second set of rainfall data contains the daily rainfall data at IAG/USP from January 1, 1931 to August 31, 2011. This dataset was used as the base of the long-term variability analysis because of its high quality (Sugahara et al. 2012), and has been used in several studies related to climate variability, climate change and extreme rainfall values (Marengo et al. 2013 and references quoted therein, Silva Dias et al. 2013). Other datasets used to explore the relationship between the various large-scale climatic patterns and rainfall over MASP (data at IAG/USP) were (1) the monthly sea surface temperature (SST) anomalies of the Japan Meteorological Agency (JMA), the SST-JMA index (www.coaps.fsu.edu/jma), (2) the PDO index (Zhang et al. 1997), (3) the Southern Annular Mode (SAM) index (Nan & Li 2003), (4) the Atlantic Multidecadal Oscillation (AMO) index (Enfield. et al. 2001), (5) the Pacific North American Oscillation (PNA) index (Wallace & Gutzler 1981), and (6) the NAO index (Hurrell 1995). The period 1951–2011 was used as a common period to ensure consistency among the different large-scale indices and rainfall data.

2.2. Spatial variability

From the daily rainfall series at distributed points (94 stations), other rainfall characteristics were derived at both annual and seasonal scales, for the period 1973–1997 (25 yr). The mean total annual (hydrological cycle, from September to August) and total seasonal values (SON, DJF, MAM and JJA) with their respective coefficients of variation (CVs); the annual mean value of the extreme rainfall events exceeding the 99th percentile of the daily rainfall (Frich et al. 2002); and the annual mean number of wet days were considered in identifying climatic spatial features of rainfall over the MASP. Also, the amplitudes and phases of the first harmonic of the monthly mean values were estimated by harmonic

Table 1. Rain gauge stations representative of the 5 regions of the Metropolitan Area of São Paulo. ANA: National Water Agency, DAEE: Department of Water and Energy of the State of São Paulo, IAG: Institute of Geophysics and Astronomy, USP: University of São Paulo. m a.s.l.: meters above (mean) sea level

Region	Latitude (S)	Longitude (W)	Altitude (m a.s.l.)	Station	Institution
North	23°38	45°57	820	Casa Grande	ANA
West	23°20	46°41	740	Franco da Rocha	DAEE
Central	23°39	46°37	799	IAG	USP
South	23°39	46°57	880	Cachoeira da Graça	DAEE
East	23°55	46°39	720	Evengelista de Sousa	DAEE

analysis (not shown here). This allows for the analyses of the rainfall variability to provide a more detailed view of the fundamental characteristics over various spatial scales and annual and seasonal timescales.

Additional rainfall analyses for the MASP were carried out with the aim of identifying the intrinsic regional features of rainfall throughout the year. These were based on the daily rainfall averages and their CVs, for the 5 stations located in different regions over MASP (Fig. 1, Table 1). The daily mean and CV values of rainfall were adequately adjusted using the smoothing method described by Mann (2008).

For evaluation of the characteristics of rainfall on spatial scales, a continuous distribution of the variable is analyzed to provide a better climatic regional-scale description and more effective spatial variability analyses. The results calculated at each station were mapped on a grid of 0.01° × 0.01° (~1.1 km) resolution using the ordinary kriging interpolation method, which assumes that the mean value is constant in the local neighborhood of each estimation point (Journel & Huijbregts 1978). The kriging method is an unbiased, optimal and linear statistical interpolation technique based on regression against observed values of surrounding data points, weighted according to spatial covariance values (Goovaerts 1997), and it has been widely used in spatial rainfall distribution estimates (Moral 2010).

2.3. Temporal variability and long-term characteristics

2.3.1. Intraseasonal and interannual variability

The wavelet transform was used to determine the dominant modes of both the intraseasonal (30–60 d) and interannual variability and their variation in time for rainfall in the MASP, through temporal multi-scale analysis. The wavelet transform is a powerful tool for time series analyses that is able to locate the variability signal simultaneously in both temporal and frequency domains. The continuous wavelet transformation; $W_n(s)$, of a time series, x_n (n = 1,…,N), is defined as the convolution of x_n with a scaled and translated version of $\psi_o(\eta)$ (Torrence & Compo 1998):

$$W_n(s) = \sum_{n'}^{N-1} x_{n'} \psi^{\star}\left[\frac{(n'-n\delta t)}{s}\right] \quad (1)$$

where the (*) is the complex conjugate, s is a scaling parameter, n is a localized time index, n' is the position along the analyzed transect, δt is the constant time interval, N is the number of pointsand ψ implies a mother wavelet. In this paper, use is made of the Morlet wavelet $\psi_o(t)$, which is a plane wave modulated by a Gaussian function expressed as:

$$\psi_o(\eta) = \pi^{-1/4} e^{i\omega_o \eta} e^{-\eta^2/2} \quad (2)$$

where i is the imaginary unit, ω_o is the non-dimensional frequency, taken equal to 6 in order to satisfy the wavelet admissibility condition (Torrence & Compo 1998) and η is the nondimensional 'time' parameter.

The intraseasonal variability of rainfall was quantified, identified and isolated in order to decompose the daily rainfall time series, as recorded at the IAG/USP station for the period January 1933–August 2011, using a wavelet transform. The wavelet transforms were calculated for every hydrological year (September–August), then scale-averaged between 30 and 60 d, to produce a time series of fractional variance in the intraseasonal frequency band, and their significance at the 95% confidence level was calculated. This broad band (30–60 d), related to the Madden–Julian Oscillation, was chosen as the dominant oscillation, based on the study of Paegle et al. (2000). For details of the scale-averaged wavelet power and the derivation of significance levels, see Torrence & Compo (1998). Thus the wavelet transform was first applied to every rainfall time series of 2 continuous years (e.g. from January 1 of Year 0 to December 31 of Year 1; ~730 d); then, the scale-averaged wavelet power between 30 and 60 d was quantified, thus specifying the intensity of the oscillations, related to the 95% confidence level. Following this process, only the statistically significant periods of intraseasonal oscillations from September 1 of Year 0 to August 31 of Year 1 (365 d) were isolated as representative throughout the hydrological annual cycle.

The dominant interannual oscillations of rainfall in the MASP were determined from the standardized monthly rainfall anomaly time series at the IAG/USP station for the period January 1933–August 2011. The standardized monthly rainfall anomaly (r_{my}) is defined as:

$$r_{my} = (R_{my} - \overline{R}_m)/\sigma_m,\ m = 1,\ldots 12;\ y = 1933,\ldots,2011 \quad (3)$$

where R_{my} is the rainfall total for month m during year y, and $\overline{R}_m$ and σ_m are the long-term mean and standard deviation of each successive month m, respectively.

2.3.2. Long-term variability

Two statistical methods are used in this study to analyze the long-term variability of rainfall time series in the MASP: (1) The non-parametric sequential Mann–Kendall test (Goossens 1983, Goossens & Berger 1987) is considered to be most appropriate for the detection of abrupt climatic change (Sneyers 1990). The standardized forward and backward variables and their levels of statistical significance were estimated following Goossens & Berger (1987). (2) The non-parametric Mann–Kendall test (Hirsch & Slack 1984, Helsel & Hirsch 1992) is used to determine the statistical significance of the trends in each of the analyzed periods, and the linear trend slopes are calculated using the non-parametric method of Sen (1968). The statistical significance of the simple monotonic trend test is determined at the 95% confidence level.

To identify rainfall trend patterns in the MASP and to establish the period and amplitude of changes in the time series over the years, repeated monotonic trend tests with variable start times (T_b) and end times (T_e) are estimated for the seasonal and annual rainfall totals recorded at the IAG/USP station, pursuant to the methodology suggested by Zhang et al. (2010). This method sheds light on rainfall variability, and is an additional tool to help to identify periods with changing trends. The initial sample interval ($T_e - T_b$) to calculate the trend pattern was 10 — which is the minimum sample that may be used by this method (Kendall 1975) — and the number of Mann–Kendall trend test calculations, N, that need to be calculated for a temporal series of rainfall of size n (years, months, seasons, days, etc.) is: $N = [(n - 8) \cdot (n - 9)]/2$. Thus, the trend pattern calculation of both the total annual (September–August) and summer (DJF) rainfall recorded at the IAG/USP station, for 1933–2010, requires the estimation of N = 2415 trends, and every value of the figure (point) represents the trend of the period between the interval ($T_e - T_b$).

2.3.3. Relationship between rainfall and large-scale circulation systems

Potential links between rainfall in the MASP and different large-scale climate patterns at seasonal and interannual scales were assessed by applying the sequential correlation coefficient of the 3-monthly means throughout the year, and the running monthly correlation for 5 yr, between the standardized monthly rainfall anomalies at the IAG/USP station and the indices of the large-scale patterns indicated in Section 2.1 for the period 1951–2011. The 5 yr period was chosen to highlight the evolution of the interannual relationship between the rainfall in MASP and the large-scale circulation, mainly for ENSO events. For this purpose, the Spearman rank correlation was used because it is robust and resistant related to the Pearson (ordinary) correlation, and it is computed from the ranks of the data rather than from the data values themselves (Wilks 2011). Because the standard t-test may overstate statistical significance due to serial correlation (or persistence), which is common for meteorological data, the statistical significance was estimated using a t-test based on an effective sample size, N_{eff}:

$$N_{eff} = N\left(\frac{1-\rho_{1x}\rho_{1y}}{1+\rho_{1x}\rho_{1y}}\right) \quad (4)$$

where N is the actual sample size and $\boldsymbol{\rho_{1x}}$ and $\boldsymbol{\rho_{1y}}$ are the lag – 1 autocorrelation coefficients of the 2 time series. The ratio $(1 + \boldsymbol{\rho_{1x}\rho_{1y}}) : (1 - \boldsymbol{\rho_{1x}\rho_{1y}})$ acts as a variance inflation factor, and it is the time between effectively independent samples (Leith 1973).

3. RESULTS

3.1. Spatial rainfall variability

The spatial distribution of the mean values of total annual rainfall, the spatial distribution of the 99th percentile, and the distribution of the mean values of wet days, computed for the period 1973–1997 are shown in Fig. 2a–c. The mean annual rainfall varied between ~1300 and ~2500 mm across the MASP, although for most of the MASP it was <1600 mm (Fig. 2a). Areas of maximum values (~2400 mm), observed along the southern side of the MASP, increase on the southeastern slope of the Serra do Mar moun-

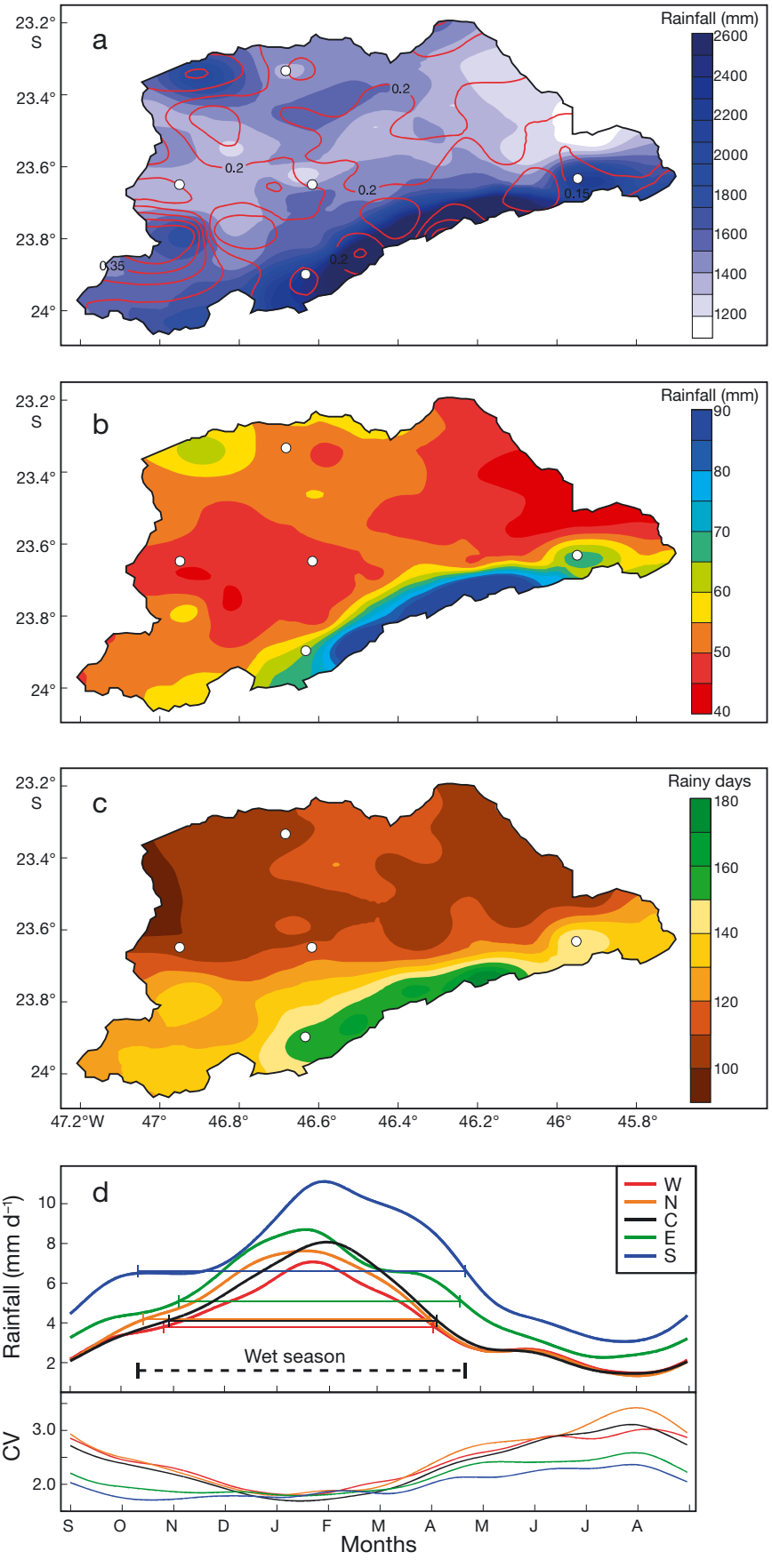

Fig. 2. Spatial distribution of (a) annual mean rainfall and coefficient of variation (CV, isolines) over the Metropolitan Area of São Paulo (MASP), (b) mean annual 99th percentile of daily rainfall, (c) annual mean number of rainy days during the year, and (d) smoothed mean daily rainfall (top) and the coefficient of variation (bottom) of the 5 stations marked on panels (a–c) (white dots) (see Table 1, Fig. 1). Each time series of (d) has been smoothed with a 30 d filter (Mann 2008). Horizontal coloured continous (dashed black lines): average duration of the rainy season in the different (all) regions of the MASP

tain range due to the ascent of moist air from the Atlantic Ocean. The 2 isolated secondary maxima located in the west are regional peculiarities forced essentially by the topographic features (Barry 2008, Houze 2012). These patterns force the establishment of the intense south–north rainfall gradient with relatively low values throughout the central region of the MASP. The spatial pattern of rainfall at seasonal scales (not shown) resembles the annual variability of rainfall, reflecting mostly the persistent influence of topography on rainfall distribution through the year.

The CV of annual rainfall over the MASP ranges from ~0.15 to ~0.30, and this spatial variability persists through all of the seasons. This pattern suggests the existence of 3 areas of relatively homogeneous rainfall variability, but with peculiar characteristics and, in large part, modulated by orographic features. These regions are:

(1) isolated areas with high values of rainfall influenced by topography and high interannual variability (CV > ~0.3), observed in the southwestern and northwestern parts of the MASP,

(2) an area with high rainfall values and low interannual variability (CV < ~0.2), modulated by the orography of the Serra do Mar mountain range, and covering the entire southern side of the MASP, and

(3) most of the MASP, where total annual rainfall is low, and the interannual variability has an intermediate CV value of ~0.2.

Fig. 2b shows that the spatial distribution of the annual mean rainfall values of the 99th percentile are close to the annual distribution (Fig. 2a). Over most of the MASP, this extreme value is <55 mm and occurs in the areas with almost homogeneous low annual values and interannual variability. However, the belt of rain values >55 mm is bounded by the orographic effects where the rainfall amounts reach high values, the highest occurring in the central part of the southern MASP (90 mm). This is consistent with the significant increase in the extreme rainfall index (95th percentile) over a great part of São Paulo state during 1950–1999 (Dufek & Ambrizzi 2007). Thus, one must be aware that the regions subject to topographic effects are more susceptible to intense rainfall events, both in the present and in a future changed climate (Marengo et al. 2013).

To further identify regions with similar numbers of wet days through the year, the annual mean of total days with rain (>1 mm) was calculated. Areas of high numbers of wet days, >150 d (~5 mo), are restricted to the southeastern portion of MASP, associated with the Sierra do Mar mountains, and numbers of wet days of <120 d (~4 mo) are observed over the rest of the domain (Fig. 2c). In addition to the above analysis, the seasonal cycle of rainfall over the MASP as depicted by the first harmonic amplitude (as a percent) and phase (month of the first harmonic in calendar months) (not presented) shows a unimodal rainfall regime with maximum values observed around late January and early February, with the peaks observed in the east slightly delayed relative to those on the southern side.

The rainfall characteristics analyzed above appear to be a consequence of the significant effect of orography on the spatial rainfall distribution characteristics in the MASP. Here it is necessary to distinguish 2 distinct aspects: (1) the Serra do Mar mountains strongly modulate the different basic characteristics of the spatial rainfall distribution in the MASP, mainly over the mountains themselves, throughout the year, taking advantage of the water vapor supplied by the Atlantic Ocean and driven by local circulation, which is the result of the complex dynamic interaction between the regional and large-scale circulation characteristics; and (2) the isolated topographic features of the MASP appear to affect only the intensity of rainfall, because over these areas the mean number of rainy days is the same, meaning that topography drives the circulation to produce strong convection, which can initiate intense local rainfall.

Regional characteristics of the seasonal rainfall development are evident along the annual cycle of mean daily rainfall and its CV in 5 stations located over the MASP (Fig. 2d). The wet season is October–April, during which the mean daily values of each region exceed the daily annual rainfall mean (Liebmann & Marengo 2001), and the maximum values occur between the end of January and the beginning of February (Fig. 2d, top), consistent with the results of the harmonic analysis. The rainy season over the MASP declines correspondingly in length as one moves farther from the southern region, with this area having an average rainy period of around 190 d (6.5 mo), with the central and western regions having rainy seasons approximately 20–30 d shorter. These variations seem to be related to the oceanic effect modulated by local topographic features (Fig. 1), corroborated by the spatial distribution of the mean annual 99th percentile of daily rainfall (Fig. 2b) and the annual mean of wet days (>1 mm) (Fig. 2c).

The results also show that over most regions of the MASP, with the exception of the southern region and to a lesser degree, the eastern portion (associated with the Serra do Mar mountain range), the cycle of daily rainfall is approximately symmetric. These cycles show a gradual increase from the driest month (July) to the wettest months (late January to early February), then they decrease gradually until the end of the rainy season (April), after which the slope becomes very weak until the driest month. On the other hand, the annual cycle of daily rainfall in the areas contiguous to the Serra do Mar mountain range (southern region) is asymmetric, with a pronounced drop in early spring, when the cycle undergoes an unexpected interruption, exactly at the beginning of the rainy season, after which the cycle continues its increasing trend with a strong slope until the wettest month (end of January). Thereafter, the decrease in rainfall is slow until the driest month (July).

The variability of the annual daily rainfall cycle derived from the CV (Fig. 2d, bottom) indicates that the dry (rainy) months have greater (lower) variability, but the southern and eastern regions have a less pronounced cycle of variability, indicating that throughout the year, precipitation occurrence is more homogeneous over these areas than in the rest of the MASP. Bearing in mind all these aspects of the annual cycle of daily rainfall, it seems that rainfall during the intermediate season months (spring and fall), particularly in the southeastern or southern MASP, are the result of underlying dynamics that are much more

complex — with the contribution of the oceanic characteristics and the ocean–atmosphere interaction in the regions adjacent to the Atlantic Ocean — than in the rest of the year, conditioned by the role played by local topography, which modulates the intensity and spatial–temporal distribution of rainfall.

The characteristics of atmospheric circulation on the mesoscale and on the synoptic scale over the MASP, which generate convective activity and its effects, seem to be more intense during spring and autumn, when the quasi-stationary frontal system known as the SACZ sporadically modulates the features of the synoptic circulation, producing frequent extreme rainfall events, as studied by Seluchi & Chou (2009), among others. The interacting local and large-scale physical and dynamic characteristics which generate the rainfall over the MASP need to be studied in regard to the diverse spatial and temporal scales of rainfall variability. Another question concerns the effect of SST of the adjacent Atlantic Ocean in increasing or reducing the amount and intensity of a given rainfall event over the MASP, given that the long-term variability of SST near the coast of São Paulo shows a positive trend over the past decades, and appears to be associated with increased rainfall at the IAG/USP station (Silva Dias et al. 2013).

3.2. Temporal variability

Due to the lack of high-quality rainfall data across the state, data from the IAG/USP station (Sugahara et al. 2012, Marengo et al. 2013) is often used as a basis to analyze the long-term climate of the MASP (Nobre et al. 2010, Silva Dias et al. 2013), allowing for a detailed temporal variability rainfall analysis.

3.2.1. Intraseasonal variability

To reveal more detailed characteristics of the intraseasonal oscillations in the MASP, this study focused on the wavelet spectrum on 30–60 d scale averages, at the 95% statistical significance level, for the daily rainfall observed at the IAG/USP station for 1933–2011 (Fig. 3). Fig. 3b shows the significant periods of the 30–60 d rainfall oscillation as vertical lines in each hydrological year (September–August). The length of the period of the oscillations observed during the year varies over the period of the analysis and apparently does not have any long-term temporal modulation (Fig. 3a). Significant intraseasonal oscillations are more frequent during the wet warm season, reaching 18 events during February (Fig. 3c), probably modulated by the activity of the SACZ (Paegle et al. 2000, Carvalho et al. 2004). In some years, this oscillation appears modulated during the wet season by both positive (1972–73) and negative (1984–85) ENSO events. Also, intense events in the intermediate seasons (spring), like that observed in 1972 and 1991, and during the winter of 1982, are associated with positive ENSO events.

The results shown here correspond only to prominent statistically significant oscillations; evidently there are other intraseasonal oscillations that occurred over the year during the period of the analyses, at the same frequency (30–60 d), with low amplitude, that do not reach statistical significance, and here those were not taken into account.

3.2.2. Interannual variability

In an exploratory analysis, we used a simple method — based on the similarity of the interannual variability of rainfall in different regions of the MASP — to reveal the most striking features of the long-term variability of rainfall in the MASP, and thus to make useful inferences about the characteristics of future precipitation.

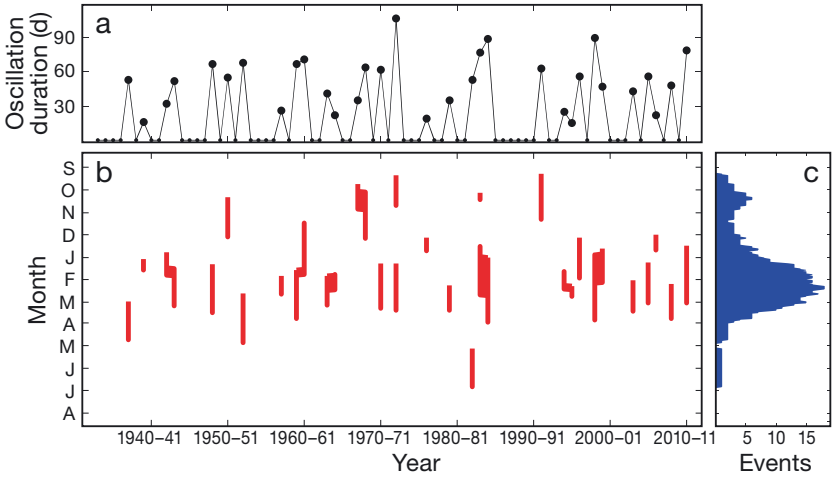

Fig. 3. Temporal distribution of the intraseasonal rainfall variability (30–60 d): (a) total duration of the oscillations, (b) period of oscillation statistically significant at 95% confidence level (vertical lines), and (c) number of events observed over the period of analysis

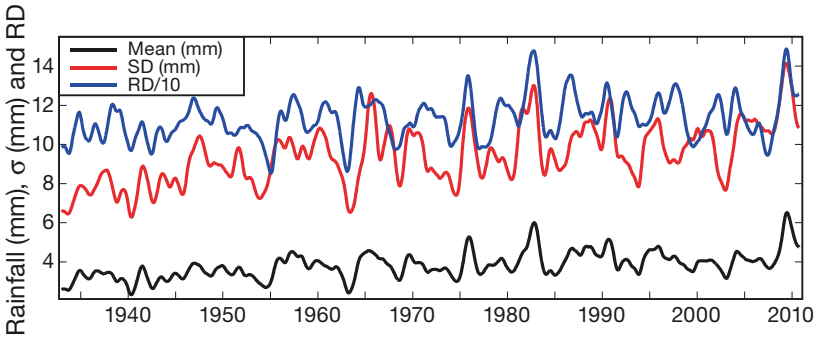

Fig. 4. Time series of the 365 d running values of mean rainfall (mm), standard deviation (SD) of rainfall and number of rain days (RD), based on daily observations from Stn IAG from January 1, 1933 through August 31, 2011. RD is divided by 10

Fig. 4 shows the mean values estimated from the average run of 365 d of total daily rainfall, the standard deviation and the frequency of rainy days (>1 mm), in the 79 yr period: January 1, 1933–August 31, 2011. Both the mean value and the standard deviation of daily rainfall increase in phase throughout the period, with starting and ending values of ~2.2 mm to ~6.8 mm and of ~6.3 σ to 14.1 σ, respectively, resulting in a positive trend of both the standard deviation (+0.4 σ decade^{-1}) and the total daily rainfall values (+0.15 mm decade^{-1}) and, at the same time, the rainy day frequency fluctuates between ~85 and ~150 d yr^{-1}, with a trend of +1.5 d decade^{-1}. The trends of all the mean values time series calculated above were statistically significant at the 95% confidence level.

These results show that the increase in rainy day frequency over time seems to account for the increase in total rainfall year after year. At the same time, the maximum or minimum values, the relative values and the standard deviation values (variability) seem to be directly related both to the average value and to the number of rainy days. In addition, high values of the mean and standard deviation increased through the years, which may explain the positive trends noted in the various extreme rainfall indices from previous studies (Dufek & Ambrizzi 2007) and in the increase in magnitude and frequency of high quantiles of daily rainfall (Sugahara et al. 2009).

To attain a deeper understanding of the long-term rainfall variability over the MASP, and identify climatic events that could explain the interannual variability, use was made of the Morlet wavelet transform analysis of standardized monthly rainfall anomalies recorded at the IAG/USP station for the period January 1933–August 2011 (Fig. 5a). The energy of the wavelet transform of standardized monthly rainfall anomalies in the MASP (Fig. 5b) shows 2 episodes of oscillations that are significant at the 95% confidence level during the analyzed period. The most notable of these oscillations appear at the interannual variability scale (2–8 yr) from 1975 to 1990; the other at the quasi-decadal variability scale (8–12 yr), taking place from the early 1950s to the early 1960s. Furthermore, the annual cycle and intra-annual variability (~1 yr) seem to be strongly associated with these oscillations. In principle, the connection between a given variability scale and other scales is the characteristic multiplicity of time scale of wavelet transforms, and this behavior is the obvious influence of the low-frequency variability upon the high-frequency variability. Thus, it is possible to affirm that the interannual and decadal precipitation oscillations influence the behavior of the annual cycle in various forms.

The interannual rainfall oscillation between 1975 and 1985 shows a strong peak between 1975 and

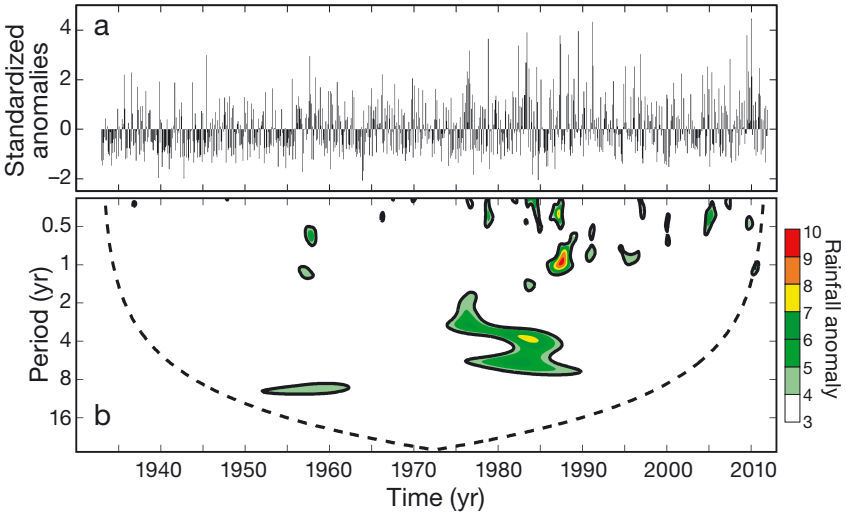

Fig. 5. (a) Time series of standardized monthly rainfall anomalies (units are standard deviations) observed at Stn IAG/USP (January 1933–August 2011), and (b) the local wavelet power spectrum of the standardized monthly rainfall anomaly. Thick contours enclose regions of >95% confidence for red-noise processes. Cone of influence is indicated by thick dashed line

1976 (1982 and 1983) during the negative (positive) phase of the ENSO phenomenon, and the spectrum value corresponding to the ENSO periods does not exceed the significance level for the global wavelet spectrum (not shown). This means that the interannual rainfall variability over the MASP can be explained by the underlying dynamics associated with this phenomenon. Although this fact explains how it is plausible that ENSO events disturb rainfall in the MASP, the relationship between the ENSO phase signal and the standardized monthly rainfall anomalies seems to be ambiguous. Due to the complexity of precipitation variability over the MASP and the weak signal/noise ratio of the impact of ENSO on this variability, the study of precipitation in different spatial and temporal scales relevant to the characterization of interannual patterns of precipitation variability and of future climate projections.

3.3. Trend patterns

The average of the total annual (September–August) and of total summer (DJF) precipitation over the period of study are, respectively, 1402 and 629 mm, with a coefficient of variation (CV) of 5.5 and 4.1 over all of the years (Fig. 6a,b, top). Over the long term, both the annual and the summer total rainfall show a positive trend of +56.4 mm decade^{-1} and +28.9 mm decade^{-1}, respectively, with statistical significance at the 95% confidence level. Further, the smoothed data analysis of both time series of precipitation have similar oscillations throughout the period, with a quasi-decadal weak amplitude oscillation before about the mid-1970s, after which the wavelength and amplitude increase over time.

Fig. 6a,b (middle) shows an abrupt climate change detected in both the annual and the summer rainfall through the period of study at the end of the 1950s. It should be noted that the abrupt changes with statistical significance at the 95% confidence level, according the sequential Mann–Kendall test, were observed after the relative rainfall magnitudes of the upward and the downward sequences functions (Goossens & Berger 1985) cross at 1957 for annual rainfall and around 1958 for summer rainfall. Moreover, after the sequence functions of the seasonal (DJF) rainfall cross, they both appear to fluctuate together around the threshold of statistical significance up to the end of the 1970s, where they become separated. This feature (together with the increase in rainfall variability observed in the smoothed time series) does not appear to be statistical evidence for the occurrence of the abrupt short climate change related to the PDO that occurred around 1976 (Zhang et al. 1997) in the MASP.

The rainfall trend patterns of the annual total and of the seasonal total of the rainy season (Fig. 6a,b, bottom) show that the domains where the slopes are statistically significant are located in the same time regions of the analyzed periods. This indicates a high degree of dependence between the total annual rainfall and total seasonal rainfall of the rainy season. According to the sign of the trend slope, a pattern of alternating positive and negative trends is noted, grouped in periods of several decades in the 2 time series, notwithstanding the fact that the greater fraction of the trend patterns is composed of positive values. This means that over relatively long periods, the total annual rainfall and the total seasonal rainfall have increased regularly since the beginning of observations in 1933, as observed principally along the left side of Fig. 6a,b (bottom), where the trends are statistically significant, mainly after 1960. The slopes grouped into periods of <~20 yr are much greater than those for longer periods and appear as a stationary quasi-decadal oscillation; the limits of its waves coincide with the period of the smoothed series (Fig. 6a,b, top). Also, the change of trend slope around the end of the 1950s in both the annual and seasonal rainfall appears to be evidence of the occurrence of the abrupt short climate change that occurred in the MASP.

3.4. Links to large-scale patterns

In this section, the seasonal and interannual evolution of the relationship between rainfall in the MASP and large-scale patterns of circulation are analyzed. Preliminary analysis of the sequential correlation among the standardized 3-month means of rainfall in the MASP and the 3-monthly means of the 6 indices of each global pattern (Section 2.1) show a weak relationship, but only the correlation among rainfall and the ENSO, PDO and SAM indices are statistically significant at the 95% confidence level in at least 1 trimester in the sequential correlation (Fig. 7a). The correlation coefficient between rainfall and the 3 indices shows a seasonal pattern, with a similar annual cycle to that of the ENSO and the PDO patterns, and opposite to that of the SAM from spring to fall. Significant direct associations between rainfall and the PDO (ENSO) are observed during the intermediate seasons (winter and beginning of the

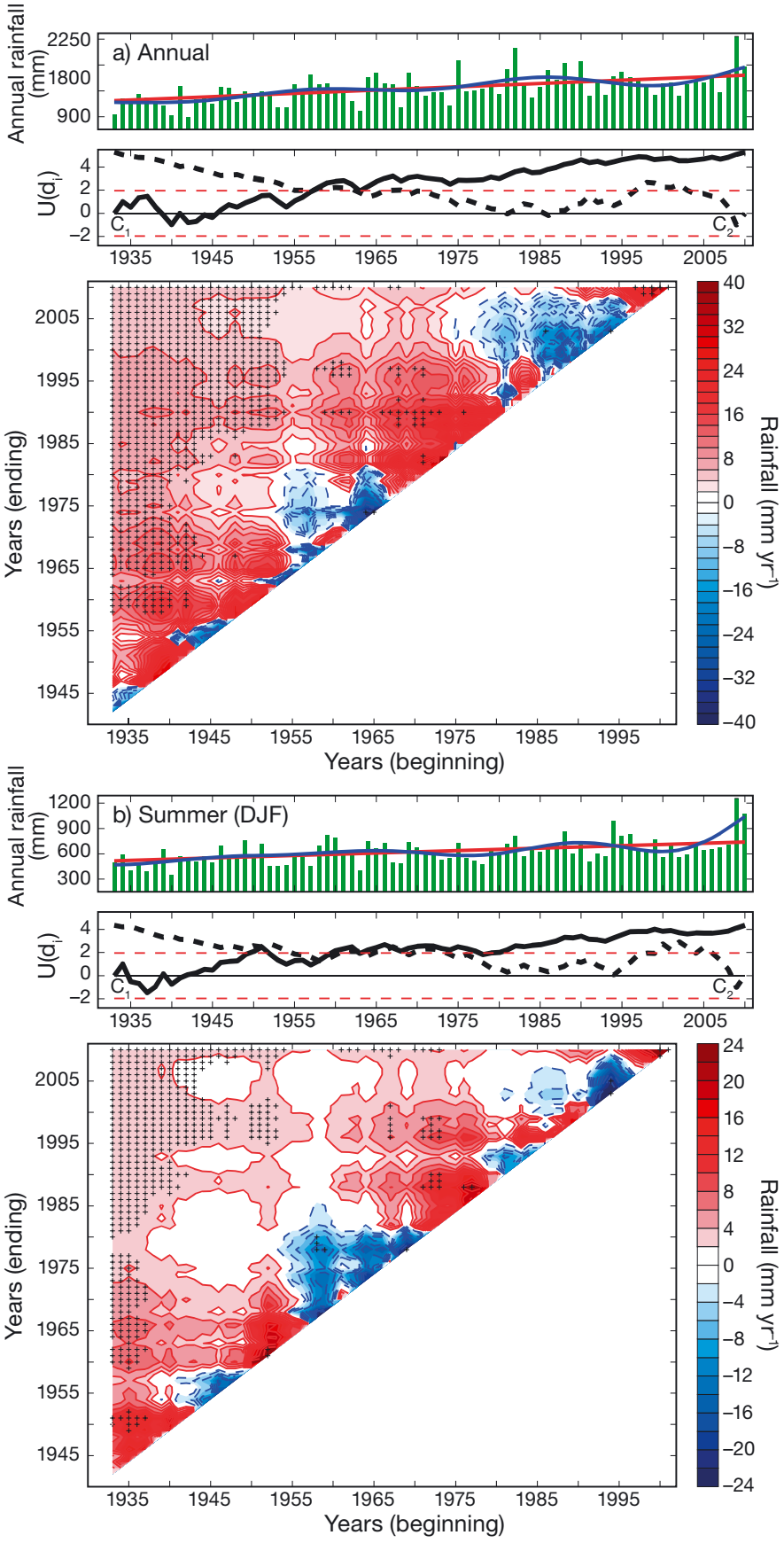

Fig. 6. (a) Temporal distribution of total annual rainfall (top), abrupt changes in total annual rainfall as derived from the sequential Mann-Kendall test ($U(d_i)$; middle) statistics and the trend pattern analysis (bottom). (b) Same as (a), but for total summer seasonal rainfall. Top: red (blue) lines correspond to the monotonic trend (25 yr smoothed time series, following Mann 2008); middle: continuous (dashed) black thick lines correspond to the forward (backward) sequential statistics, C_1 (C_2) sequential statistics, and horizontal dashed red lines correspond to confidence limits at 95% significance level (±1.96 sigma); bottom: horizontal (vertical) axis indicates the beginning (end) of the variable period used to calculate the trend. Hatched areas indicate significant trends at 95% significance level

rainy season), SON and MAM (JJA and ASO). Also, a significant correlation is observed between rainfall and the SAM index during the DJF rainy season. Thus, the magnitude of the correlation patterns indicates that the different large-scale circulation patterns exert a weak direct control of the driving dynamic.

The correlation runs of 60 mo (5 yr) show evidence that only extreme anomaly periods of the 3 global patterns affect rainfall in the MASP in either a direct or inverse relationship (Fig. 7b). From these patterns, the SAM appears to be most reliable relationship, having significant correlation, and it can cause both positive and negative anomalies of rainfall over the MASP in accord with the anomaly of the SAM. This fact is associated with the opposite phases of the SAM, which modulates the high-latitude transient waves rather than stationary waves (Lorenz & Hartmann 2001) driven by the entrance of extratropical high-frequency systems (synoptic waves) into South America, reaching Southeast Brazil. Furthermore, the effects of the ENSO (PDO) on rainfall over the MASP appear to be ambiguous (weak) at interannual scales. Also, the significant direct association between rainfall and ENSO

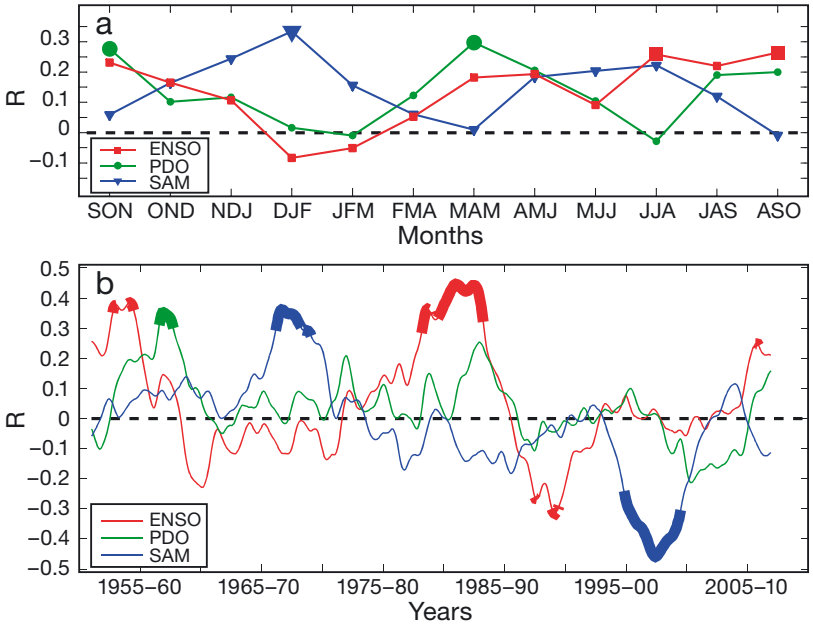

Fig. 7. (a) Three-month sequential correlation, and (b) 5 yr running monthly correlation between rainfall and the El Niño–Southern Oscillation (ENSO), Pacific Decadal Oscillation (PDO) and Southern Annular Mode (SAM) indices. Large filled marks indicate statistical significance at 95% confidence level in (a). Bold lines identify period with correlation significant at 95% confidence level in (b)

observed by the end of the 1950s appears related to the quasi-decadal scales of the rainfall (Fig. 5b).

4. CONCLUSIONS

In the MASP region, as in many other regions of the world, lack of high-quality rainfall data makes it difficult to perform any reliable spatial analyses of rainfall variability, because these kinds of analyses require detailed information of rainfall distribution in both space and time over a long period of time. In this study, from all the available data scattered over all of the MASP (110 stations), for the period 1933–2002, we choose daily rainfall time series recorded at 94 gauge stations for the period 1973–1997 to investigate spatial analyses over the MASP. Previously, we applied a quality control method for daily rainfall inconsistencies. From these daily times series, rainfall statistics (e.g. total, mean, standard deviation, etc.) were computed and spatially mapped on a grid of 0.01° × 0.01° (1.1 km) resolution by the kriging interpolation method.

The spatial distribution of the annual cycle of rainfall over the MASP was examined based on the analysis of daily rainfall in 5 stations for the period 1973–1997, and the long-term variability and trend patterns (Zhang et. al. 2010) were computed based on annual and on rainy season (DJF) time series of the IAG/USP station for a 79 yr period (1933–2011). Thus, it is hoped that the results of these analyses will contribute to the knowledge of rainfall variability in the MASP, and that future studies will aid understanding of the spatial–temporal rainfall variability in relation to the local physical and dynamic effects and the large-scale factors responsible for rainfall occurrence in the MASP.

The spatial distribution of the mean annual rainfall shows low values over the entire central part of the MASP on an almost east–west axis, flanked by high rainfall values along the southeast side modulated strongly by the orography of the Serra do Mar, and by isolated centers of high rainfall, related to isolated topographic features, in the western side of the MASP forced by portion of the Serra da Cantareira and Serra da Paranapiacaba, respectively. These features can be ascribed to the prominent spatial distribution of both the extreme rainfall pattern (99th percentile) and the number of wet days in the year. In addition, the length of the rainy season varies along the MASP, with periods of >6.5 months in the southern region to periods of ~5.5 months around the central and western regions; it is evident that during the intermediate seasons, the physical mechanisms that cause the rainfall are more complex, and the non-linear interactions among topography and local and large-scale circulation, and the water vapor supplied by the adjacent Atlantic Ocean, are stronger than in other seasons.

Results of the intraseasonal variability, determined by 30–60 d oscillation (statistically significant at the 95% confidence level) of the scale-average wavelet power clearly show high interannual variability without a long-term modulation. It is more frequent during summer, peaking in February (18 events in 78 years), and is strongly related to the occurrence of the SACZ (Silveira & Siva Dias 1990). Also, it is evident that the ENSO in either its negative or positive phase appears to drive this oscillation during the transitional seasons, as was observed in spring of 1972 and 1991 (beginning of the rainy season), and in

the unique long-lasting and intense event at the beginning of the strong 1982–1983 ENSO event, between May and June of 1982 (dry season). Additionally, the analyses of interannual variability, as carried out by means of the wavelet transform method, reveal that the effect of the ENSO phenomenon on rainfall variability is plausible but complex, and subject to the life cycle of each ENSO event.

A comparison of the temporal evolution of the mean and standard deviation of daily precipitation and number of rainy days exhibits a continuous increase over the years from 1933 on; this is a very significant indication that rainfall became more intense, and extreme rainfall more frequent, as the years went by. This shows that any discussion regarding the urban effect's influence on rainfall is potentially problematic due to record sampling limitations and high rainfall variability, since a single storm event can affect all of the statistics. In that sense, the sequential Mann–Kendall statistics showed a significant abrupt change in long-term rainfall variability in the MASP at the end of the 1950s. Some peculiar temporal characteristics observed after the middle of the 1970s seem to indicate the possible effects, mainly in the rainfall variability, of a large-scale abrupt climate change that occurred in 1976, associated with the PDO (Zhang et al. 2010). The trend patterns showed statistically significant trends at the 95% confidence level in total annual and seasonal rainfall in the rainy season (DFJ) for periods of >~30 years that are all positive, mainly after 1960, but they unmistakably reveal the constant increase in rainfall in the MASP since 1930, when rainfall records at the IAG/USP station started. Strong negative trends of short periods are clustered around the occurrence of the abrupt climate change at the end of the 1950s in both annual and seasonal rainfall. However, the large-scale abrupt climatic change observed in the middle of the 1970s is not evident in both annual and seasonal rainfall.

Finally, the weak magnitude of the correlation between rainfall in the MASP and the various indices of large-scale atmospheric circulation patterns shows that rainfall variability in MASP is not explicitly modulated by change in large-scale circulation. However, the weak relationship though statistically significant between rainfall and the SAM, ENSO and PDO indices at seasonal scales, seems to be a decisive factor altering the normal progression of the seasonal rainfall cycle. At interannual scales, each one of these circulation patterns drives rainfall variability, mainly when each pattern reaches its extreme value.

Acknowledgements. G.O.O. was supported in part by the National Institute of Science and Technology for Climate Change (INCT-CC) under CNPq grant 573797/2008-0 and FAPESP Grant 2008/57719-9, and the FAPESP-Assessment of Impacts and Vulnerability to Climate Change in Brazil and Strategies for Adaptation Options project (Ref. 2008/58161-1). J.A.M. was supported by the Brazilian National Council for Scientific and Technological Development (CNPq). Additional funding was provided by Rede-CLIMA, the National Institute of Science and Technology for Climate Change (INCT-CC), FAPESP-grant Assessment of Impacts and Vulnerability to Climate Change in Brazil and strategies for Adaptation options project (Ref. 2008/58161-1), FAPESP-NERC grant Impacts of Climate Extremes on ecosystems and human health in Brazil: PULSE-Brazil (Ref. 2011/51843-2), and FAPESP-GO AMAZON grant 2013/50538-7. This work was partially funded by the UK Strategic Programme Fund (SPF) throughout the study 'Vulnerability of Brazilian Megacities to Climate Change: Metropolitan Areas of São Paulo and Rio de Janeiro'. Constructive suggestions and comments from the anonymous reviewers helped in improving the manuscript.

LITERATURE CITED

Ahmed K, Sanches E (eds) (2008) Strategic environmental assessment for policies: an instrument for good governance. World Bank, Washington, DC

Alexander LV, Zhang X, Peterson TC, Caesar J and others (2006) Global observed changes in daily climate extremes of temperature and precipitation. J Geophys Res 111:D05109, doi:10.1029/2005JD006290

Barros AP (1994) Dynamic modeling of orographically induced precipitation. Rev Geophys 32:265–284

Barry RG (2008) Mountain weather and climate. Cambridge University Press, New York, NY

Carvalho LMV, Jones C, Liebmann B (2004) The South Atlantic Convergence Zone: intensity, form, persistence, and relationships with intraseasonal to interannual activity and extreme rainfall. J Clim 17:88–108

Donat MG, Alexander LV, Yang H, Durre I and others (2013) Updated analyses of temperature and precipitation extreme indices since the beginning of the twentieth century: the HadEX2 dataset. J Geophys Res Atmos 118: 2098–2118

Dufek AS, Ambrizzi T (2007) Precipitation variability in Sao Paulo State, Brazil. Theor Appl Climatol 93:167–178

Einfalt T, Michaelides S (2008) Quality control of precipitation data. In: Michaelides S (ed) Precipitation: advances in measurement, estimation and prediction. Springer-Verlag, Berlin, p 101–126

Enfield DB, Mestas-Nunez AM, Trimble PJ (2001) The Atlantic Multidecadal Oscillation and its relationship to rainfall and river flows in the continental U.S. Geophys Res Lett 28:2077–2080

Freitas ED, Rozoff CM, Cotton WR, Silva Dias PL (2007) Interactions of an urban heat island and sea breeze circulations during winter over the Metropolitan Area of São Paulo - Brazil. Boundary-Layer Meteorol 122:43–65

Frich P, Alexander LV, Della-Marta P, Gleason B, Haylock M, Klein Tank AMG, Peterson T (2002) Observed coherent changes in climatic extremes during the second half of the twentieth century. Clim Res 19:193–212

Goossens C (1983) Etude de l'homogeneite et de la stabilite

des series climatiques. Scientific Report 19831. Universite Catholique de Louvain, Louvain

Goossens C, Berger A (1987) How to recognize an abrupt climatic change. In Berger WH, Labeyrie LD (eds) Abrupt climate change: evidence and implications. Kluwer, Dordrecht, p 31–46

Goovaerts P (1997) Geostatistics for natural resources evaluation. Oxford University Press, New York, NY

Groisman PY, Knight RW, Easterling DA, Karl TR, Razuvaev VN (2005) Trends in intense precipitation in the climate record. J Clim 18:1326–1350

Helsel DR, Hirsch RM (1992) Statistical methods in water resources. Elsevier Science, New York, NY

Hirsch RM, Slack JR (1984) A non-parametric trend test for seasonal data with serial dependence. Water Resour Res 20:727–732

Houze RA Jr (2012) Orographic effects on precipitating clouds. Rev Geophys 50:RG1001, doi:10.1029/2011RG000365

Hurrell JW (1995) Decadal trends in the North Atlantic Oscillation: regional temperatures and precipitation. Science 269:676–679

IBGE (Instituto Brasileiro de Geografía e Estatística) (2011) Sinopse do censo demográfico 2010. IBGE, Rio de Janeiro. Available at: http://portal.mte.gov.br/data/files/8A7C816A2E7311D1013003524D7B79E4/IBGE_CENSO2010_sinopse.pdf

Journel AG, Huijbregts CJ (1978) Mining geostatistics. Academic Press, London

Kane RP (2000) Relationships between El Niño timings and rainfall extremes in NE Brazil, São Paulo City and south Brazil. Rev Bras Meteorol 15:45–57

Katz RW, Brown BG (1992) Extreme events in a changing climate: variability is more important than averages. Clim Change 21:289–302

Kendall MG (1975) Rank correlation methods, 4th edn. Charles Griffin, London.

Landsberg HE (1981) The urban climate. International Geophysics Series, Vol 28. Academic Press, New York, NY

Leith C (1973) The standard error of time-average estimates of climatic means. J Appl Meteorol 12:1066–1069

Liebmann B, Marengo JA (2001) Interannual variability of rainy season and rainfall in Brazilian Amazon basin. J Clim 14:4308–4318

Lorenz DJ, Hartmann DL (2001) Eddy-zonal flow feedback in the Southern Hemisphere. J Atmos Sci 58:3312–3327

Magaña V, Perez J, Mendez M (2003) Diagnosis and prognosis of extreme precipitation events in the Mexico City Basin. Geofis Int 41:247–259

Mann ME (2008) Smoothing of climate time series revisited. Geophys Res Lett 35:L16708, doi:10.1029/2008GL034716

Marengo JA, Jones R, Alves LM, Valverde M (2009) Future change of temperature and precipitation extremes in South America as derived from the PRECIS regional climate modeling system. Int J Climatol 29:2241–2255

Marengo JA, Valverde MC, Obregón GO (2013) Observed and projected changes in rainfall extremes in the Metropolitan Area of São Paulo. Clim Res 57:61–72

Marquina A (2010) Global warming and climate change: prospects and policies in Asia and Europe. Palgrave Macmillan, London

Min S, Zhang KX, Zwiers F, Hegerl GC (2011) Human contribution to more-intense precipitation extremes. Nature 470:378–381

Moral FJ (2010) Comparison of different geostatistical approaches to map climate variables: application to precipitation. Int J Climatol 30:620–631

Nan S, Li J (2003) The relationship between summer precipitation in the Yangtze River valley and the previous Southern Hemisphere Annular Mode. Geophys Res Lett 30:2266, doi:10.1029/2003GL018381

Nobre CA, Young AF, Salvida P, Marengo JA and others (2010) Vulnerabilidade das megacidades Brasileiras ás mudanças climáticas: Região Metropolitana de São Paulo. INPE/UNICAMP/USP/IPT/UNESP, INPE, São José dos Campos

Paegle JN, Byerle LA, Mo KC (2000) Intraseasonal modulation of South American summer precipitation. Mon Weather Rev 128:837–850

Pall P, Aina T, Stone DA, Stott PA and others (2011) Anthropogenic greenhouse gas contribution to flood risk in England and Wales in autumn 2000. Nature 470:382–385

Parry ML, Canziani OF, Palutikof JP, Adger N and others (2007) Technical summary. In: Parry ML, Canziani OF, Palutikof JP, van der Linden PJ, Hanson CE (eds) Climate change 2007: impacts, adaptation and vulnerability. Contribution of Working Group II to the Fourth Assessment Report of the Intergovernmental Panel on Climate Change. Cambridge University Press, Cambridge, p 23–78

Pereira Filho AJ, Haas R, Ambrizzi T (2002) Caracterização de eventos de enchente na bacia do Alto Tietê por meio do radar meteorológico e da modelagem numérica de mesoscala. Anais do XII Congresso Brasileiro de Meteorologia, Foz do Iguaçu, Paraná, 04–11 August2002, (CD-ROM)

Pereira Filho AJ, Barros MTL, Hallak R, Gandu AW (2004) Enchentes na Região Metropolitana de São Paulo: aspectos de mesoescala e avaliação de impactos. Anais do XIII Congresso Brasileiro de Meteorologia, Fortaleza, Ceará, 29 August–03 September 2004, (CD-ROM)

Reboita MS, Gan MA, Rocha RP, Ambrizzi T (2010) Regimes de precipitação na América do Sul: uma revisão bibliográfica. Rev Bras Meteorol 25:185–204

Ronchi C, Rabuffetti D, Salandin A, Vargiu A, Barbero S, Pelosini R (2007) Development of the Piedmont Region Hydrological Bulletin as a support to water resources monitoring and management. In: Rossi G et al. (eds) Methods and tools for drought analysis and management, Book 62. Water Science and Technology Library. Springer, Dordrecht, p 49–65

Seluchi ME, Chou SC (2009) Synoptic patterns associated with landslide events in the Sierra do Mar, Brazil. Theor Appl Climatol 98:67–77

Sen PK (1968) Estimates of the regression coefficient based on Kendall's tau. J Am Stat Assoc 63:1379–1389

Silva Dias MAF, Silva Dias J, Carvalho LMV, Freitas ED, Silva Dias PL (2013) Changes in extreme daily rainfall for São Paulo, Brazil. Clim Change 116:705–722

Silveira RB, Silva Dias MAF (1990) Análise dos ecos de radar de São Paulo durante o EM-III – diagnóstico de superfície e estudo de precipitação. In anais do VI Congresso Brasileiro de Meteorologia, Salvador, Bahia, 19–23 November 1990, p 738–742

Sneyers R (1990) On the statistical analysis of series of observations. WMO Tech Note 143. WMO No. 415:TP-103. WMO, Geneva

Sugahara S, da Rocha RP, Bomfim R (2009) Non-stationary frequency analysis of extreme daily rainfall in Sao Paulo, Brazil. Int J Climatol 29:1339–1349

Sugahara S, da Rocha RP, Ynoue RY, Bomfim R (2012) Homogeneity assessment of a station climate series (1933–2005) in the Metropolitan Area of São Paulo: instruments change and urbanization effects. Theor Appl Climatol 107:361–374

Torrence C, Compo GP (1998) A practical guide to wavelet analysis. Bull Am Meteorol Soc 79:61–78

Wallace JM, Gutzler DS (1981) Teleconnections in the geopotential height field during the Northern Hemisphere winter. Mon Weather Rev 109:784–812

Westra S, Alexander LV, Zwiers FW (2013) Global increasing trends in annual maximum daily precipitation. J Clim 26:3904–3918

Wilks DS (2011) Statistical methods in the atmospheric sciences, 3rd edn. Academic Press, San Diego, CA

Xavier TMBS, Xavier A, Silva Dias MAF (1994) Evolução da precipitação diária num ambiente urbano: o caso da cidade de São Paulo. Rev Bras Meteorol 9:44–53

Xavier TMBS, Silva Dias MAF, Xavier AFS (1995) Impact of ENSO episodes on the autumn rainfall patterns near São Paulo, Brazil. Int J Climatol 15:571–584

Zhang Y, Wallace JM, Battisti DS (1997) ENSO-like interdecadal variability: 1900-93. J Clim 10:1004–1020

Zhang Z, Dehoff AD, Pody RD (2010) New approach to identify trend patterns of streamflows. J Hydrol Eng 15: 244–248

Editorial responsibility: Helmut Mayer, Freiburg, Germany; Matthias Seaman, Oldendorf/Luhe, Germany

Submitted: August 22, 2012; Accepted: May 8, 2014
Proofs received from author(s): August 27, 2014